Accepted Manuscript

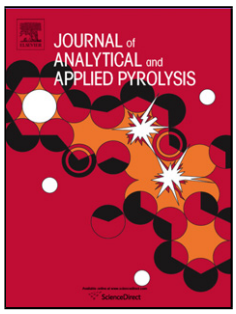

Title: Pyrolysis and combustion study of flexible polyurethane foam

Author: M.A. Garrido R. Font

PII: S0165-2370(14)00367-2
DOI: http://dx.doi.org/doi:10.1016/j.jaap.2014.12.017
Reference: JAAP 3369

To appear in: *J. Anal. Appl. Pyrolysis*

Please cite this article as: M.A.Garrido, R.Font, Pyrolysis and combustion study of flexible polyurethane foam, Journal of Analytical and Applied Pyrolysis http://dx.doi.org/10.1016/j.jaap.2014.12.017

Pyrolysis and combustion study of flexible polyurethane foam

M.A. GARRIDO, R. FONT*

University Institute of Engineering of Chemical Processes, University of Alicante, P.O. Box 99, E-03080 Alicante

*Email: mangeles.garrido@ua.es

Abstract

The thermal degradation of flexible polyurethane foam has been studied under different conditions by thermogravimetric analysis (TG), thermogravimetric analysis-infrared spectrometry (TG-IR) and thermogravimetric analysis-mass spectrometry (TG-MS). For the kinetic study, dynamic and dynamic+isothermal runs were performed at different heating rates (5, 10 and 20 ºC min^{-1}) in three different atmospheres (N_2, N_2:O_2 4:1 and N_2:O_2 9:1). Two reaction models were obtained, one for the pyrolysis and another for the combustion degradation (N_2:O_2 4:1 and N_2:O_2 9:1), simultaneously correlating the experimental data from the dynamic and dynamic+isothermal runs at different heating rates. The pyrolytic model considered consisted of two consecutive reactions with activation energies of 142 and 217.5 kJ mol^{-1} and reaction orders of 0.805 and 1.146. Nevertheless, to simulate the experimental data from the combustion runs, three consecutive reactions were employed with activation energies of 237.9, 103.5 and 120.1 kJ mol^{-1}, and reaction orders of 2.003, 0.778 and 1.025. From the characterization of the

sample employing TG-IR and TG-MS, the results obtained showed that the FPUF, under an inert atmosphere, started the decomposition breaking the urethane bond to produce long chains of ethers which were degraded immediately in the next step.

However, under an oxidative atmosphere, at the first step not only the urethane bonds were broken but also some ether polyols started their degradation which finished at the second step producing a char that was degraded at the last stage.

Keywords: Polyurethane; Kinetics; Pyrolysis; Combustion; Thermogravimetric.

Nomenclature table

α_i	Conversion degree in the reaction i
DTG_{max}	Maximum value in the Derivative Thermogravimetric curve
E_i	Activation energy for the reaction i
FPUF	Flexible Polyurethane Foam
k_i	Kinetic constant for the reaction i
K_i*	Compatible kinetic constant for the reaction i
k_{i0}	Pre-exponential factor of the Arrhenius equation for the reaction i
k'_{i0}	Pre-exponential factor of the Arrhenius equation corrected with the effect of the oxygen for the reaction i
MDI	Methyl Diphenyl Diisocyanate
n_i	Reaction order for the reaction i
N_{total}	Total number of experimental data employed in the optimisation
P	Number of optimised parameters
P_{O2}	Partial pressure of oxygen in the atmosphere
PU	Polyurethane
R	Gas constant (J mol^{-1} k^{-1})
TDI	Toluene Diisocyanate
TG	Thermogravimetric analysis
TG-IR	Thermogravimetric analysis-infrared spectrometry
TG-MS	Thermogravimetric analysis-mass spectrometry
T_{ref}	Temperature around the maximum decomposition rate
$\upsilon_{i\,inf}$	Mass fraction of volatiles that can be obtained at infinity time from the reaction i
V_{exp}	Average of the experimental mass fraction of volatiles
V_i	Mass fraction of volatiles at any time in the reaction i

1. Introduction

Polyurethanes (PUs) are one of the most useful commercial polymers which are widely used in both industry and everyday life applications. Furniture, particularly mattresses

and interior industry, dominates the polyurethane market accounting for 28.01% of the total demand in 2010. The most common destination for end-of-life mattresses appears to be landfilled. However, mattresses account for a large proportion of the total waste sent to landfill because of their small density (10% by volume according to one study for the South East of England). This represents a large quantity of material which is not recovered.

The repeating unit in the polyurethanes is the urethane bond $(-NH-COO-)$ obtained from the reaction between an isocyanate $(-N=C=O)$ and an alcohol $(-OH)$. The most used raw material components of polyurethane foams are polyethers and polyesther polyols, methyl diphenyl diisocyanate (MDI) and toluene diisocyanate (TDI) [1]. In addition, a variety of additives, blowing agents and water are added. Two different blowing agents are employed to the solidifying plastic, carbon dioxide and methylene chloride. While the carbon dioxide is produced in the reaction between the water and the isocyanate group, the methylene chloride (CH_2Cl_2) is added as a supplementary blowing agent [2].

Pyrolysis and combustion mechanisms and the characterization of polyurethane polymers have been studied by other authors previously. Herrera et al. [3] used thermogravimetric analysis-mass spectrometry (TG-MS) and thermogravimetric analysis coupled with fourier transformed infrared spectroscopy (TG-FTIR) to study the evolved gas analysis in the thermal degradation of the rigid polyurethane foam in a N_2 atmosphere, and they also characterized the products from the combustion and pyrolysis of samples (about 40 mg) in an oven by gas chromatography-mass spectrometry (GC-

MS) and high performance liquid chromatography analysis with fluorescence detection (HPLC-FD).

Another group of additives, which has been studied by different authors, are the fire retardants which are added to the polymer to stop or retard the burning process. Wang et al. [4] synthesized polyurethanes with different amounts of flame retardant poly(bispropoxyphosphazene) to study the thermal degradation behavior of these polyurethanes with TG and TG-FTIR. Gao et al. [5] applied laser pyrolysis and time-of-flight mass spectrometry to the study of rapid thermal degradation of rigid polyurethane foams with different ranges of isocyanate and fire retardants. They deduced that the polypropylene glycol was the major flammable compound evolved during laser pyrolysis and the concentration of this compound in the volatiles reduced when the amount of isocyanate increased.

Chao and Wang [6] compared the effect of phosphorus and brominated fire retardants in thermal decomposition processes setting the different degradation steps in air and nitrogen, and also proposing thermal degradation mechanisms for the polyurethane.

Rogers and Ohlemiller [7] studied the thermal decomposition of a flexible polyurethane foam based on TDI and a polyether polyol of propylene oxide with the TG technique. In nitrogen atmosphere the decomposition proceeded in two overall steps. At the end of the first step the cellular structure collapsed to a viscid liquid which decomposed further in agreement with a random nucleation rate law. The activation parameters provided similar patterns to the experimental TG curves at heating rates of 2 and 20 ^{o}C min^{-1}.

Day et al. [8] carried out an interesting study on the effect of copper, iron and dirt in the thermal degradation of PU. The results suggested that the presence of metal

contamination in this polymer could influence the thermal degradation. Specifically, it was found that certain metal contaminants could have a catalytic effect on the degradation processes.

Bilbao et al. [9] determined the kinetic equations of polyurethane foam weight loss and analysed the influence of the atmosphere, using nitrogen and air with a TG apparatus. They also related the results of the kinetic constants obtained from isothermal and dynamic experiment.

Font et al. [10] studied the thermal decomposition of a polyurethane based adhesive in an inert atmosphere, using different apparatus, a thermobalance and a laboratory furnace to study the kinetics of decomposition and the evolution of gaseous products, respectively. The experimental results were described satisfactorily by a two-parallel reaction model and the kinetic parameters, that is, the pre-exponential factors, activation energies, reaction orders and maximum production of volatiles at an infinite time were also obtained. Gas chromatography-mass spectrometry (GC-MS) was used to identify volatile and semivolatile organic compounds generated by the thermal degradation reactions.

The main aim of this paper has been to propose two models to describe the pyrolysis and combustion degradation of flexible polyurethane foam (FPUF) wastes. In order to obtain a single set of kinetic parameters for pyrolysis and combustion, a wide range of runs were performed in each condition. In addition, the evolution of some compounds during the decomposition has been observed employing TG-MS and TG-IR.

2. Experimental

2.1. Raw material

The FPUF studied was obtained from the mattresses disposed of in a landfill in Alicante, Spain. The moisture of the polyurethane foam used was 1.2% and the density was 19.62 kg m^{-3}, the value was within the range proposed by the Polyurethane Foam Association for mattress topper pads and upholstery [11].

Elemental analysis, determined in a Perkin-Elmer 2400 apparatus, and the Net Calorific Value determined using an AC-350 LECO Calorimetric Bomb, are shown in Table 1. Table 2 also shows the weight percentage obtained from the semi-quantitative analysis of the containing elements, performed by X-ray fluorescence with an automatic sequential spectrometer (model TW 1480, Philips Magix Pro, Philips Co., Ltd.).

For the analysis of chlorine in the FPUF, the EPA Method 5050 followed by EPA Method 9056 was used. The foam is oxidized by combustion in the bomb previously indicated, and the evolved chloride is adsorbed in a sodium carbonate/sodium bicarbonate solution. A small volume of collection solution is injected into an ion chromatography with a conductivity detector (Dionex DX-500, Thermo Fisher Scientific). The average concentration obtained from this analysis in triplicate was 253 mg of chloride per kg of dry mass (0.0253%). This chloride could come from the methylene chloride (CH_2Cl_2) which is used as blowing agent [2].

In order to characterize the real composition of the FPUF, the functional chemical groups were identified by attenuated total reflection-Fourier transform infrared (ATR-FTIR) spectroscopy (BRUKER IFS 66/S). The ATR-FTIR was equipped with a single reflection Golden Gate accessory with a diamond crystal. The spectra were recorded within the range of 600–4500 cm^{-1} with a resolution of 1 cm^{-1}.

The spectrum obtained is shown in Error! Reference source not found. The FTIR spectra shows that the isocyanate (-NCO) absorption band centered at 2230 cm^{-1} is clearly missing while the presence of the amide absorption band (N-H) at 3294 cm^{-1}, carbonyl urethane group (C=O) centered around 1719 cm^{-1} and the carbamate group (CN-H) at 1641 cm^{-1} indicates the urethane linkage in the polyurethane [12]. This fact confirms that almost all of the diisocyanate groups reacted during the polymerization and formed urethane linkages and amide groups. On the other hand, the (C-O-C) asymmetric stretching peak at 1223 cm^{-1} and the (C-O-C) symmetric stretching peak at 1092 cm^{-1} represent the aliphatic ether, which confirm that a polyether polyol was used as raw material instead of polyesther polyol. The peak at 1534 cm^{-1} symbolises the (C-N) stretching and the (N-H) in plane bending of the Amide II, while the peaks at 1411 cm^{-1} and 1597 cm^{-1} are characteristic of the aromatic ring from diisocyanate. Finally, the peaks centered at 2971 cm^{-1} and 2868 cm^{-1} are assigned to symmetric and asymmetric stretching mode (C-H) in CH_2 and the peak 1373 cm^{-1} is characteristic of the out of plane bending mode (C-H) in CH_2 [13].

Figure 1.

2.2. Apparatus

2.2.1. Thermogravimetric analysis (TG)

The thermogravimetric analysis (TG) was performed employing two different apparatus. For the pyrolysis runs a TGA/SDTA-6000 Perkin Elmer Thermobalance was employed. This apparatus has a vertical furnace and a single beam vertical balance. The flow rate of nitrogen gas was 100 cm^3 min^{-1}. Sample weights were around 7.5 mg.

The combustion runs were carried out in a Setaram TG-DTA 92-16.18 Thermobalance. Two atmospheres were employed for the study of combustion degradation consisting of a mixture of nitrogen and oxygen with two different ratios: N_2:O_2 4:1 and N_2:O_2 9:1, both with a flow rate of 100 cm^3 min^{-1}.

Dynamic experiments were carried out at different heating rates of 5, 10 and 20 ºC min^{-1}, from 30 ºC to a final temperature of 900 ºC.

Dynamic+isothermal experiments were also carried out. These experiments started with a constant heating rate until the set temperature was obtained, and then, the final temperature was maintained constant throughout the pyrolysis or combustion process for a long period of time. The final temperatures were selected to cover all the decomposition range observed in the dynamic experiments.

2.2.2. Thermogravimetric analysis-mass spectrometry (TG-MS)

For the Thermogravimetric-mass spectrometry analysis (TG-MS) a TGA/SDTA851e/LF/1600 coupled to a Thermostar GSD301T Pfeiffer Vacuum MS apparatus was employed. Operating conditions common in all runs were: weight sample around 5 mg, heating rate 30 ºC min^{-1}, ionization 70 eV and SIR (selected ion recording) detection of several ions during two different runs. In the first run the required ions were (m/z): 4, 13–18, 25–32, 35–46 and in the second run they were (m/z): 4, 32, 43–46, 50–52, 55–58, 60, 65, 68, 73, 78, 91, 96, 105, 106. He and He:O_2 (4:1) gases were employed to perform both pyrolytic and oxidative decomposition.

2.2.3. Thermogravimetric analysis-infrared spectrometry (TG-IR)

The thermogravimetric analysis-infrared spectrometry (TG-IR) of the FPUF was performed using a Perkin-Elmer STA6000 and a Nicolet 6700 FT-IR using nitrogen and

air as carrier gases. About 8 mg of sample was put in a crucible and was heated from 25 to 600ºC with a heating rate of 30 ºC min^{-1}. The absorbance was measured from 4000 to 600 cm^{-1}.

3. Results and discussion

3.1. Initial mass effect

Figure 2 shows the TG results for FPUF with a heating rate of 10 ºC min^{-1} but with different initial mass, between 5 to 10 mg in inert atmosphere (N_2). In this figure, the weight fraction represents the ratio between the instantaneous sample mass (including residue formed and non-reacted initial solid) and the initial sample mass. In view of

Figure 2, it is deduced that the initial value mass has a very small effect in the decomposition process. It can also be confirmed that FPUF appeared to degrade in two stage processes [8], one around 275 ºC and the other around 380 ºC, but

Figure 2 also shows another weight loss around 700 ºC. The foam obtained from the landfill was not clean and $CaCO_3$ can be a part of this dirt, as it can be confirmed observing Table 2, where the Ca accounts for 9% of dry weight of the sample. The $CaCO_3$ decomposes around 700 ºC to obtain CaO and CO_2 [14], consequently, the thermal degradation studies for FPUF have been carried out up to 600 ºC, to consider only the organic fraction. The weight loss due to CO_2 obtained from $CaCO_3$ degradation is around 5% of the total weight loss.

Figure 2

3.2. Analysis of data obtained from the TG-IR.

The TG and DTG curves, obtained in the TG-IR experiments carried out at 30 ºC min^{-1} in nitrogen and air atmosphere, are shown in **Figure 3**. It can be observed that the FPUF decomposes in two steps for an inert atmosphere, with DTG_{max} at 300 and 397 ºC and in three steps for air atmosphere with DTG_{max} at 300, 339 and 550ºC.

Figure 3.

Figure 4 shows the IR spectra obtained at the maximum temperature of evolution rates, 300 and 397 ºC, in nitrogen atmosphere. At the first step, Figure 4(A), of the thermal degradation (300 ºC) the following peaks of the volatiles evolved can be observed: the symmetric and asymmetric characteristic stretching vibration of N─H at 3357 cm^{-1}, the stretching vibration of ─CH_2─ groups at 2931 cm^{-1} and the symetric and asymetric band of C─O─C in aryl alkyl ethers account for the peaks at 1056 cm^{-1} and 1217 cm^{-1}. Furthermore, the formation of CO_2 is confirmed by the peak at 2360 cm^{-1}, although another peak should have been detected around 2310 cm^{-1}, although its vibration region overlapped with ─NCO vibration region (around 2275 cm^{-1}) [15]. Other peaks are located between 3400-3900 cm^{-1} and 1303-1625 cm^{-1} which suggest the presence of water vapours in the thermal decomposition gases [16]. These peaks indicate that the thermal degradation of FPUF in an inert atmosphere starts with the break of urethane bonds at low temperature. Rupture of hard segments is in accordance with the formation of great amounts of isocyanates (─NCO) and water vapor [17].

On the other hand, at the second step Figure 4(B), of thermal degradation (397 ºC) the peaks at 2973 cm^{-1}, 2931 cm^{-1} and 2877 cm^{-1} are associated to the stretching vibration of ─CH_3, ─CH_2 and ─CH, respectively, and these peaks increase greatly with the temperature [18]. The other products exhibit the characteristic bands of CO_2 at 2366 cm^{-1}

and 2327 cm^{-1} and the presence of carbonyl group in esters (─C═O) at 1745 cm^{-1}. Thus, the peaks at 910 cm^{-1}, 1375 cm^{-1} and 1452 cm^{-1} also indicate the formation of tert-butyl groups (─C─$(CH_3)_3$), in addition to the presence of different types of ethers shown by the peaks at 1662 cm^{-1} for the vinyl ethers, and the peaks at 1022 cm^{-1} and 1278 cm^{-1} for the symetric and asymetric absortion band of C─O─C in aryl alkyl ethers [17]. Finally, the strongest absorption peak is detected at 1108 cm^{-1}, which is due to the stretching vibration of C─O─C bond from ethers with high polarity. Therefore, in the second stage of the thermal degradation, the ether polyols obtained in the first stage, are decomposed to products with methyl, methylene, methine, C─O─C and carbonyl groups, and CO_2.

Figure 4.

Figure 5 shows the IR spectra obtained at two maximum temperature of evolution rates, 300 and 339 ºC, in air. At the first step, Figure 5(A), of thermal degradation (DTG_{max1} at 300 ºC) the peaks detected at 669 cm^{-1}, 2321 cm^{-1} and 2362 cm^{-1} are characteristics of the formation of CO_2, while the presence of absorption bands at 1376-1558 cm^{-1} and 3400-3900 cm^{-1} is attributed to water vapor [16]. The gaseous products evolved for FPUF at 300ºC also exhibit characteristic bands of stretching vibration C-O-C groups from ethers at 1000-1313 cm^{-1}, carbonyl group in esters (─C═O) at 1745 cm^{-1} [17] and stretching vibration C-H at 2800-3000 cm^{-1} [19]. There are new bands, compared with those obtained in the pyrolysis experiment, such as 2111 cm^{-1} and 2167 cm^{-1} attributed to CO due to the excess of O_2 in the atmosphere [19].

Figure 5.

At the second step, Figure 5(B), of the thermal degradation of FPUF in an oxidative atmosphere, the presence of CO_2 was also detected as the main gas with the peaks at 669

cm^{-1}, 2331 cm^{-1} and 2364 cm^{-1} [16]. Furthermore, the characteristic absorption bands of 3400-3900 cm^{-1} for water vapor [16], 1083 cm^{-1} and 1220 cm^{-1} for stretching vibration C-O-C groups from ethers [17] and 2881-2973 cm^{-1} stretching vibration C-H [19] have also been detected in this degradation stage. New peaks have been obtained at 339 ºC as the blend vibration N-H at 1531 cm^{-1} and 1592 cm^{-1} [20], vinyl ethers at 1692 cm^{-1} and symmetric and asymmetric stretching vibration N-H at 3355 cm^{-1} [17].

The TG-IR spectra obtained at the third step (550ºC) show that CO_2 and CO are the only peaks detected which are the products from the combustion char.

Therefore, in the first stage of thermal degradation in N_2 atmosphere the most abundant gaseous products are those with isocyanate groups. At the second step of pyrolysis, part of the products from the first stage are degraded to obtain, mainly, ─C═O and hydrocarbon (─CH_3, ─CH_2 and ─CH) compounds. Nevertheless, with air the compounds evolved from the first step are mainly with ─C═O groups and CO_2, and from the second step H_2O, CO_2 and some minority ─N─H compounds are obtained.

3.3. Analysis of data obtained from the TG-MS

Figure 6 shows the variation of the intensity of some ions corresponding to water (ion 18), to hydrogen cyanide (ion 27) and to carbon dioxide (ion 44) in helium and helium:oxygen 4:1 for FPUF carried out at 30 ºC min^{-1}.

The decomposition of FPUF under an inert atmosphere took place in two main steps (Figure 6(A)) 280 and 380 ºC while the degradation in an oxidative atmosphere occurred in three stages (Figure 6(B)) 280, 340 and 540 ºC. There is a clear evolution of hydrogen cyanide (ion 27) at the second step of the thermal degradation under inert atmosphere (coming from the decomposition of the diisocyanate) as reported in other studies [21]

which cannot be obtained in the oxidative decomposition. Water has been detected in both, inert and oxidative atmosphere, the intensity of this peak is greater in He:O_2 4:1 than in He. The residual water and dioxide carbon in the helium run is a consequence of the interaction of the product evolved and retained inside the transfer line with small quantities of oxygen in the helium stream.

Figure 6.

As reported in other studies, it is possible to assume that during the degradation of FPUF in air (or synthetic air in this case), the third step corresponds to the combustion of the small fraction of carbon formed in the previous step [22] with only CO_2 (ion 44) as the main evolving product.

Concerning the graphs obtained studying the evolution of all the ions indicated previously (section 2.2.2.) during the pyrolysis of FPUF, in addition to **Figure 6**, it can be profiled that there is an evolution of formaldehyde (ions 28, 29 and 30), acetaldehyde (ions 29 and 43), ethane (ions 26, 27, 28 and 30), ethylene (ions 26 and 27), acetylene (ions 25 and 26), other hydrocarbons (ions 25, 26, 27, 39, 40, 41 and 42) and other oxygenated compounds (ions 43, 45 and 46). The emissions of aromatic compounds such as benzene, toluene and xylene (ions 78, 91 and 106) have also been detected in the thermal degradation of FPUF in an inert atmosphere. Similar results have been obtained in the thermal degradation in He:O_2 (4:1) atmosphere

The evolution of ions 35 and 36 characteristic of HCl has been studied, which can be related with the formation of chlorinated compounds in pyrolysis and combustion processes. In the case of the thermal degradation in helium atmosphere, the emission of HCl is rather small. Nevertheless, in He:O_2 atmosphere the evolution of HCl cannot be observed, so this indicates that its formation is very small.

3.4. Analysis of data obtained from the TG

Figure 7 shows the experimental TG and Derivative TG (DTG) curves for FPUF at heat rates of 5, 10 and 20 ºC min^{-1}. with 7.5 mg initial mass in nitrogen atmosphere.

Figure 7.

In addition, TG-DTG runs were carried out in nitrogen atmosphere with dynamic+isothermal conditions. **Figure 8** shows the curves obtained indicating the heating rate during the first period until reaching the temperature which is maintained constant during the isothermal period. Note that for these types of experiments the value of the weight fraction has been represented versus the time and not versus the temperature, because these runs take place in isothermal conditions.

Figure 8.

In view of the previous Figures, it can be deduced that the thermal degradation of the FPUF in an inert atmosphere could be analysed regarding two fractions, with the first decomposition step at about 280 ºC and the second at about 370 ºC.

Figure 9 and **Figure 10** show the experimental results obtained in the atmosphere N_2:O_2 4:1 for dynamic and dynamic+isothermal conditions.

Figure 9.

Figure 10.

Figure 11 and **Figure 12** show the experimental results obtained in the atmosphere N_2:O_2 9:1 for dynamic and dynamic+isothermal conditions.

Figure 11.

Figure 12.

In this case, with an oxidative atmosphere, the FPUF presents three maximums of the decomposition rates approximately 280, 340 and 500 ºC. These maximums can be seen

most clearly in the curves from the N_2:O_2 9:1 atmosphere (**Figure 11**) than those obtained under a more oxidative atmosphere such as N_2:O_2 4:1 (**Figure 9**). Normally, each maximum is associated with decomposition of a fraction or decomposition step. Three steps were also obtained by other authors [23,24] who established that the first step corresponds to the decomposition of the urethane bond to obtain isocyanate monomers and polyols segments which are degraded during the second stage. The last step, about 500ºC, is the decomposition of the residue obtained in the previous stage to obtain the same final residue as that obtained in the pyrolysis decomposition. It means that at 600ºC, all the organic fraction in the FPUF has been degraded independently of the atmosphere employed.

Comparing the curves from inert and oxidative experiments carried out at 10ºC/min (**Figure 13**), it can be observed that there is a concordance between pyrolysis and combustion at the first part, a difference in the second part and a new step appears at high temperatures in the combustion experiments (around 550ºC) related with the char combustion.

Furthermore, the second step, where the polyols segments are decomposed, is accelerated by the presence of the oxygen in the atmosphere. Consequently, the temperature of this stage is lower when the concentration of oxygen in the atmosphere increases.

Figure 13.

3.5. Kinetic model

3.6.1. Pyrolysis

By analyzing the TG results in nitrogen atmosphere, **Figure 7** and **Figure 8**, it can be observed that, at least, two pyrolysis reactions are taking place. Two consecutive pyrolytic reactions (**Scheme 1.**) are considered, in which the solid products obtained in the first reaction are degraded in the second reaction:

$$foam \xrightarrow{1} \left(1 - v_{1\inf}\right) products_1 + v_{1\inf} volatiles_1$$

$$\left(1 - v_{1\inf}\right) products_1 \xrightarrow{2} \left(1 - v_{2\inf}\right) residue + v_{2\inf} volatiles_2$$

Scheme 1.

where $v_{1\inf}$ is the mass fraction of volatiles that can be obtained at infinity time from the reaction 1 and $v_{2\inf}$ is the mass fraction of volatiles of reaction 2.

The conversion degree in each reaction is defined as the ratio between the mass fraction of volatiles at any time (V_i) and the mass fraction of volatiles at infinity time ($v_{i\inf}$), so:

$$\alpha_i = \frac{V_i}{v_{i\inf}} \quad i = 1,2 \qquad (1)$$

The kinetic expressions performed in this model, follow the kinetic law for solid decomposition proposed by Font et al [25]. For the reaction 1 it can be written as:

$$\frac{d\left(V_1 / v_{1\inf}\right)}{dt} = \frac{d\alpha_1}{dt} = k_1 \left(1 - \alpha_1\right)^{n_1} \qquad (2)$$

and for reaction 2, as it is a consecutive reaction, the kinetic expression is:

$$\frac{d\left(V_2 / v_{2\inf}\right)}{dt} = \frac{d\alpha_2}{dt} = k_2\left(\alpha_1 - \alpha_2\right)^{n_2} \quad (3)$$

It is assumed that the kinetic constant follows the usual Arrhenius dependence on temperature:

$$k_i = k_{i0}\exp\left(\frac{-E_i}{RT}\right) \quad i = 1,2 \quad (4)$$

The volatiles obtained in each time, *V*, can be related to the conversion degrees, α_1 and α_2, by equation 5.

$$V = \left(V_1 + V_2\right) = \left(v_{1\inf}\alpha_1 + v_{2\inf}\alpha_2\right) \quad (5)$$

Conversely, from the TG analysis, the volatiles in each time can be calculated with the equation (6):

$$V_{\exp} = 1 - w_{\exp} \quad (6)$$

With the intention of obtaining a single set of parameters for the pyrolysis, the dynamics runs and dynamic+isothermal runs were correlated together.

The calculated values were obtained by integration of the differential equations presented previously by the Euler method. To minimize the differences between the experimental and calculated volatiles, we used the optimisation method of Solver function in Excel.

Two objective functions were considered, where all data obtained at different heating rates are included.

First objective function:

$$O.F._1 = \sum_{m=1}^{M}\sum_{j=1}^{J}\left[\left(\frac{dV}{dt}\right)_{\exp_{m,j}} - \left(\frac{dV}{dt}\right)_{cal_{m,j}}\right]^2 \quad (7)$$

Second objective function:

$$O.F._2 = \sum_{m=1}^{M}\sum_{j=1}^{J}\left[(V)_{\exp_{m,j}} - (V)_{cal_{m,j}}\right]^2 \quad (8)$$

where M is the number of heating rates runs studied and J is the number of points in each run. This objective function was chosen to correct the effect of the different time derivatives of V at different heating rates. With this function the contribution of all the experiments in the objective function is similar.

In order to improve the convergence, and according to the previous study [26], the optimisation was performed in terms of a "compatible kinetic constant" K_i^* instead of optimise k_{0i}.

$$K_i^* = k_i\,(0.64)^{n_i} = \left(k_{i0}\exp\left(\frac{-E_i}{RT_{ref}}\right)\right)(0.64)^{n_i} \quad (9)$$

where T_{ref} is a temperature around the maximum decomposition rate and k_{i0} is calculated from the optimised parameters K_i^*, n_i and E_i.

To validate this model the variation coefficient (VC) was calculated with the following equation:

$$VC = \frac{\sqrt{OF/\left(N_{Total} - P\right)}}{\overline{V_{\exp}}} \quad (10)$$

where N_{Total} is the number of experimental data employed in the optimisation, P are the parameters fitted, and $\overline{V_{exp}}$ is the average of the experimental volatiles.

The three dynamic and three dynamic+isothermal runs carried out in nitrogen atmosphere have been correlated together. The correlation parameters are shown in Table 3:

The calculated results obtained using the kinetic parameters shown in the **Table 3** (black line in **Figure 7** and **Figure 8**) concur extremely closely with the experimental ones.

In view of the Table 3, it can be observed that in the second reaction the mass of volatiles is higher than in the first reaction. Note that dynamic+isothermal runs were carried out to obtain a general model and decrease the great interrelation between the kinetic parameters.

A number of articles have estimated the kinetic properties of flexible polyurethane foam decomposition in nitrogen atmosphere using different kinetic models that in most cases consist of two consecutive reactions, at least. In Table 4 the results obtained from the literature are shown. It can be seen that the values of the kinetic parameters obtained in this study do not concur with those published in previous papers, which can be a consequence of the types of experiments employed for the kinetic study: dynamic and dynamic+isothermal. The trend of activation energy and pre-exponential factor observed in the kinetic parameters obtained in this study concurs with those proposed by Day et al. [8] and Prasad et al. [27], where these parameters are greater in the second reaction than in the first one.

In most of the previous papers, the reaction order considered was 1 for the both the reactions, which is not really different from that the values optimised in this study. However, Prasad et al. [27] considered the reaction orders as other kinetic parameters and the results obtained were close to those which we propose.

3.6.2. Combustion

The model proposed for the thermo-oxidative degradation of FPUF is presented in **Scheme 2** where three consecutive reactions have been considered. The first reaction for this model is a pyrolytic reaction, as in the pyrolysis model, but a new set of parameters have been optimised for these conditions. Conversely, the second and third reactions include the effect of oxygen, which is responsible for the fact that the second degradation stage came on to lower temperatures than in the pyrolysis runs.

$$foam \xrightarrow{1} \left(1-v_{1\text{inf}}\right) products_1 + v_{1\text{inf}}\, volatiles_1$$

$$\left(1-v_{1\text{inf}}\right) products_1 + O_2 \xrightarrow{2} \left(1-v_{2\text{inf}}\right) char + v_{2\text{inf}}\, volatiles_2$$

$$\left(1-v_{2\text{inf}}\right) char + O_2 \xrightarrow{3} \left(1-v_{3\text{inf}}\right) ash + v_{3\text{inf}}\, volatiles_3$$

Scheme 2

The kinetic equations for the two oxidative reactions were defined as:

$$\frac{d\left(V_2 / v_{2\text{inf}}\right)}{dt} = \frac{d\alpha_2}{dt} = k_2'\left(\alpha_1 - \alpha_2\right)^{n_2} \qquad (11)$$

$$\frac{d\left(V_3 / v_{3\text{inf}}\right)}{dt} = \frac{d\alpha_3}{dt} = k_3'\left(\alpha_2 - \alpha_3\right)^{n_3} \qquad (12)$$

Note that in the previous equations the kinetic constants are defined as k_2' and k_3', in order to include the effect of the oxygen in the model. For this reason, the pre-exponential factor was defined as the combination of two terms; the first, the typical Arrhenius pre-exponential factor and, the second, the partial pressure of oxygen in the atmosphere raised to the power of the reaction order for the oxygen for these equations (see equation 13):

$$k'_{i,0} = k_{i,0}\left(P_{O_2}\right)^{b_i} \quad i = 2,3 \qquad (13)$$

where P_{O_2} is 0.20 and 0.10 atm for the atmospheres N_2:O_2 4:1 and N_2:O_2 9:1, respectively.

The total volatiles calculated in this model were:

$$V = \left(V_1 + V_2 + V_3\right) = \left(v_{1\text{inf}}\,\alpha_1 + v_{2\text{inf}}\,\alpha_2 + v_{3\text{inf}}\,\alpha_3\right) \qquad (14)$$

With the same expression for the objective functions that were employed in the pyrolysis, and using a compatible kinetic constant (K_i^*) to improve the convergence, the three dynamic runs and the three dynamic+isothermal runs carried out in N_2:O_2 4:1 and N_2:O_2 9:1 atmospheres, were correlated together, and after the optimisation process, the correlation parameters are shown in Table 5:

The variation coefficient obtained is small, a value of 3.16%, taking into account that twelve different runs were simultaneously correlated with the same set of parameters.

The calculated and experimental weight loss curves have been plotted together in previous figures (**Figure 9** to **Figure 12**), where it can be seen that the experimental results were satisfactorily correlated.

In spite of the complex thermal degradation behavior of polyurethane foam, previous reports stated that the mechanism consisted of only a few global reactions. Ohlemiller et al. [29] proposed a two-step mechanism inside a physical-chemical model for the

smoldering combustion through the porous bulk of a flexible polyurethane, consisting of the oxidative degradation of fuel to produce char and the subsequent oxidation of char (activation energies 140 and 126 kJ mol^{-1}, respectively). Dosanjh et al. [30] simplified the description of the mechanism using a one-step reaction for the complete smoldering combustion of uniform polyurethane cylinder with the activation energy of 155 kJ mol^{-1}.

Table 6 shows some kinetic parameters proposed by authors with the characteristics of each study and considering only the kinetic decomposition.

NFR: Non-fire retardant; FR: Fire retardant; $\upsilon_{\beta,1}$**:** mass yield of specie β-foam per mass the reactant in reaction 1; $\upsilon_{c,2}$**:** mass yield of specie char per mass the reactant in reaction 2; $\upsilon_{r,5}$**:** mass yield of specie residue per mass the reactant in reaction 5Bilbao et al. [9] employed the experimental data from one dynamic run of 5ºC/min in air to study the kinetic of thermal degradation and they considered that this degradation occurred between 230 and 300ºC. For this interval, they employed the Arrhenius equation to optimise the kinetic parameters. Chao and Wang [6] suggested a three step mechanism to describe the thermal degradation for FPUFs with three pyrolytic reactions in TG analysis. Branca et al. [24] studied the oxidative degradation of a rigid polyurethane foam under four different heating rates to obtain the kinetic parameters of three consecutive pyrolytic reactions where the reaction order for each reaction was one. After that, Rein et al. [31] proposed three reactions, two competitive reactions of oxidation and pyrolysis and the consecutive char oxidation, to simulate the experimental data from one dynamic run of 10ºC/min. The scheme considered by Rein et al. [31] is similar to the scheme selected in this study; nevertheless, the optimised parameters obtained in each case are different. The reaction order (n_i) and the activation energy have the same trend in both studies and the optimised values are similar, but the pre-exponential factor, the reactor order for the oxygen and the mass fraction of volatiles present important differences which can be a consequence of the scheme selected and the experimental data employed to do the correlation; the rang of experimental conditions considered in this study is more extensive than in the previous study.

The most complex mechanism was developed by Rein et al. [23] which considered that the thermal degradation of FPUF followed a five-step mechanism consisting of four competitive reactions of oxidation and pyrolysis for the raw material (*foam*) and the product from the pyrolysis of the foam (*β–foam)*, and the final char oxidation.

- Pyrolysis of solid species *foam* to species *β–foam*
- Pyrolysis of solid species *β–foam* to *char*
- Oxidation of the solid species *foam* to *char*

- Oxidation of the solid species *β–foam* to *char*
- Oxidation of the *char* to *ash*

They employed the thermogravimetric data from a single dynamic experiment with a heating rate of 20ºC/min and a genetic algorithm to obtain the kinetic parameters shown in **Table 6.** As can be observed in **Table 6**, they assumed that reactions 3 and 4 (the oxidation reactions of *foam* and *β-foam*) have the same kinetic parameters in order to obtain a mechanism as simple as possible. In this case, the comparison between the optimised parameters in each study is difficult due to the different schemes selected.

The kinetic model proposed in this study was obtained taking into account two different atmospheres and inside each atmosphere, the experimental data from six experiments both dynamic and dynamic+isothermal conditions. Therefore, this model can be applied to a great variety of experimental data and a wide interval of operating conditions.

4. Conclusions

Regarding the pyrolysis runs, a kinetic model with two consecutive reactions has been deduced. The experimental data of the 3 dynamic runs and 3 dynamic+isothermal runs can be simulated with the potential model for the two consecutive reactions, with apparent activation energies of 142 and 217.5 kJ/mol and reaction order of 0.805 and 1.146, respectively. It has been tested that the first decomposition step corresponds to the break of the urethane bond to obtain mainly isocyanates. In the second step however, the decomposition of ether polyols takes place, forming a residue similar to the ash formed in combustion

In the combustion runs, carried out with two atmospheres of N_2:O_2 4:1 and 9:1, the kinetic model deduced is based on three consecutive reactions, satisfactorily simulating

the experimental results of 12 runs (3 dynamic runs and 3 dynamic+isothermal runs for each atmosphere). The activation energies and reaction orders are 237.9, 103.5 and 120.1 kJ/mol and 2.003, 0.778 and 1.025, respectively. The orders with respect to the oxygen are 1.114 and 0.571 for the second and third reaction, respectively. It has been tested, that the first reaction corresponds to the degradation of urethane bonds and part of the polyol segments, which means that the degradation is accelerated by the presence of oxygen in the atmosphere. The second reaction is a decomposition of ether polyols that leads to the char formation, and the third reaction corresponds to the combustion of the previous char formed.

Acknowledgment

The authors thank the Spanish Ministry of Education Culture and Sport and the research projects CTQ2013-41006 from the Spanish Ministry of Economy and Competitiveness and PROMETEOII/2014/007 from the Valencian Community Government for the support provided.

References

[1] D.K. Chattopadhyay and D.C. Webster, *Progress in Polymer Science*, 34, (2009) 1068.
[2] J.E. Packer, J. Robertson and H. Wansbrough, *Chemical Processes in New Zealand*, New Zealand Institute of Chemistry, 1998, p.
[3] M. Herrera, M. Wilhelm, G. Matuschek and A. Kettrup, *Journal of Analytical and Applied Pyrolysis*, 58–59, (2001) 173.
[4] P.-S. Wang, W.-Y. Chiu, L.-W. Chen, B.-L. Denq, T.-M. Don and Y.-S. Chiu, *Polymer Degradation and Stability*, 66, (1999) 307.
[5] F. Gao, D. Price, G.J. Milnes, B. Eling, C.I. Lindsay and P.T. McGrail, *Journal of Analytical and Applied Pyrolysis*, 40–41, (1997) 217.
[6] C.Y.H. Chao and J.H. Wang, *Journal of Fire Sciences*, 19, (2001) 137.
[7] F.E. Rogers and T.J. Ohlemiller, *Journal of Macromolecular Science: Part A - Chemistry*, 15, (1981) 169.
[8] M. Day, J.D. Cooney and M. MacKinnon, *Polymer Degradation and Stability*, 48, (1995) 341.
[9] R. Bilbao, J.F. Mastral, J. Ceamanos and M.E. Aldea, *Journal of Analytical and Applied Pyrolysis*, 37, (1996) 69.
[10] R. Font, A. Fullana, J.A. Caballero, J. Candela and A. Garcia, *Journal of Analytical and Applied Pyrolysis*, 58, (2001) 63.

[11] PFA, in *InTouch Technical Bulletins* Loudon, New Hampshire, USA, 1991.
[12] Chee Sien Wong and K.H. Badri, *Materials Sciences and Applications*, 3, (2012) 78.
[13] Y.-C. Tu, Polyurethane foam from novel soy-based polyols, University of Missouri, Faculty of the Graduate School, 2008,
[14] Y.S. M. Mustakimah, M. Saikat, *Journal of Engineering Science and Technology*, 7, (2012) 1.
[15] H.H.G. Jellinek and K. Takada, *Journal of Polymer Science: Polymer Chemistry Edition*, 15, (1977) 2269.
[16] D. Rosu, N. Tudorachi and L. Rosu, *Journal of Analytical and Applied Pyrolysis*, 89, (2010) 152.
[17] L.L. Jiao, H.H. Xiao, Q.S. Wang and J.H. Sun, *Polymer Degradation and Stability*, 98, (2013) 2687.
[18] X.L. Chen, L.L. Huo, C.M. Jiao and S.X. Li, *Journal of Analytical and Applied Pyrolysis*, 100, (2013) 186.
[19] J.M. Cervantes-Uc, J.I.M. Espinosa, J.V. Cauich-Rodríguez, A. Ávila-Ortega, H. Vázquez-Torres, A. Marcos-Fernández and J. San Román, *Polymer Degradation and Stability*, 94, (2009) 1666.
[20] X. Qian, L. Song, Y. Hu, R.K.K. Yuen, L. Chen, Y. Guo, N. Hong and S. Jiang, *Industrial & Engineering Chemistry Research*, 50, (2011) 1881.
[21] D.A.G. Purser, P. , *Fire and Materials* 8, (1984) 10.
[22] M. Herrera, G. Matuschek and A. Kettrup, *Polymer Degradation and Stability*, 78, (2002) 323.
[23] G. Rein, C. Lautenberger, A.C. Fernandez-Pello, J.L. Torero and D.L. Urban, *Combustion and Flame*, 146, (2006) 95.
[24] C. Branca, C. Di Blasi, A. Casu, V. Morone and C. Costa, *Thermochimica Acta*, 399, (2003) 127.
[25] R. Font, I. Martín-Gullón, M. Esperanza and A. Fullana, *Journal of Analytical and Applied Pyrolysis*, 58-59, (2001) 703.
[26] I. Martín-Gullón, M.F. Gómez-Rico, A. Fullana and R. Font, *Journal of Analytical and Applied Pyrolysis*, 68–69, (2003) 645.
[27] K. Prasad, R. Kramer, N. Marsh, M. Nyden, T. Ohlemiller and M. Zammarano, *Numerical simulation of fire spread on polyurethane foam slabs*, at: Proceedings of the 11th international conference on fire and materials. Interscience Communications, London, 697.
[28] D.S.W. Pau, C.M. Fleischmann, M.J. Spearpoint and K.Y. Li, *Journal of Fire Sciences*, 31, (2013) 356.
[29] T.J. Ohlemiller, J. Bellan and F. Rogers, *Combustion and Flame*, 36, (1979).
[30] S.S. Dosanjh, P.J. Pagni and A.C. Fernandez-Pello, *Combustion and Flame*, 68, (1987) 131.
[31] G. Rein, A. Bar-Ilan, A.C. Fernandez-Pello, J.L. Ellzey, J.L. Torero and D.L. Urban, *Proceedings of the Combustion Institute*, 30, (2005) 2327.

LIST OF CAPTIONS

FIGURES

Figure 1. The ATR-FTIR spectrum of Flexible Polyurethane Foam (FPUF).

Figure 2. Influence of the initial mass in the weight loss vs temperature for a run carried out at 10 ºC min^{-1} in N_2 atmosphere.

Figure 3. TG and DTG curves of FPUF in N_2 (A) and Air (B) atmosphere at 30 ºC min^{-1}.

Figure 4. IR spectra of FPUF obtained at maximum decomposition rates, 300ºC (A) and 397ºC (B), in N_2 atmosphere at 30 ºC min^{-1}.

Figure 5. IR spectra of FPUF obtained at maximum decomposition rates, 300ºC (A) and 339ºC (B), in air atmosphere at 30 ºC min^{-1}.

Figure 6. Variation of intensity of some ions and weight fraction vs temperature for the runs carried out at 30 ºC min^{-1} in He (A) and He:O_2 (4:1) (B) (ion 18, ion 27 and ion 44).

Figure 7. TG and DTG curves for dynamic runs carried out at different heating rates in N_2 atmosphere.

Figure 8. TG and DTG curves for three dynamic+isothermal runs in N_2 atmosphere.

Figure 9. TG and DTG curves for dynamic runs carried out at different heating rates in N_2:O_2 (4:1) atmosphere.

Figure 10. TG and DTG curves for three dynamic+isothermal runs carried out in N_2:O_2 (4:1) atmosphere.

Figure 11. TG and DTG curves for dynamic runs carried out at different heating rates in N_2:O_2 (9:1) atmosphere.

Figure 12. TG and DTG curves for three dynamic+isothermal runs carried out in N_2:O_2 (9:1) atmosphere.

Figure 13. Experimental data from the thermal degradation at 10ºC min^{-1} at three different atmospheres (N_2, N_2:O_2 (4:1) and N_2:O_2 (9:1)).

Table 1 Elemental analysis and net calorific value of FPUF.

Composition on dry weight basis	
C (%)	57.79
H (%)	7.36
N (%)	5.95
S (%)	<0.01
Ash (%)	5.47
O (%) per difference	23.43
Net calorific value	5786 kcal kg dry mass^{-1}

Table 2. X-Ray analysis of the material employed.

Elements	Dry weight percentage (%)
Ca	9.19
O	3.87
Si	0.105
Sn	0.105
Cl	0.0385
Na	0.0273
Fe	0.0247
S	0.0127

Mg	0.0097
Al	0.00797
P	0.00157

Table 3 Optimised parameters for pyrolysis of FPUF.

	Reaction 1	*Reaction 2*
k_0 (s^{-1})	2.044 x 10^{11}	3.247 x 10^{15}
E (kJ mol^{-1})	142.0	217.5
n	0.805	1.246
v_{inf}	0.307	0.582
VC(%)	1.79	

Table 4 Optimised parameters for pyrolysis of FPUF [28]

ference	**Scheme**	**Experiments**	**Pre-exponential factor (s^{-1})**		**Activation Energy (kJ mol^{-1})**		**Reaction order**		**Vo in**
nd Ohlemiller [29]	2 Consecutive reactions	4 Dynamic runs (2, 5, 10 and 20ºC/min)	k_{10}	5.67x10^{17}	E_1	218	n_1	1.00	v_{i}
			k_{20}	1.13x10^{11}	E_2	163	n_2	1.00	v_{i}

et al. [8]	2 Consecutive reactions	5 Dynamic runs (0.5, 1, 2, 5 and 10ºC/min)	k_{10}	$1.23x10^{13}$	E_3	122	n_1	1.00	v_i
			k_{20}	$8.511x10^{16}$	E_4	181.6	n_2	1.00	v_i
o et al. [9]	3 Consecutive reactions	1 Dynamic run (5ºC/min) (Compared with isothermal data)	k_{10}	$6.50x10^{-1}$	E_1	28.7	n_1	1.00	v_i
			k_{20}	$1.78x10^{3}$	E_2	63.1	n_2	1.00	v_i
			k_{30}	$1.57x10^{12}$	E_3	180	n_3	1.00	v_i
nd Wang [6]	2 Consecutive reactions	3 Dynamic runs (5, 10 and 20ºC/min) Kinetic parameters for each heating rate	$k_{10,NFR}$	$1.00x10^{2}$ - $2.34x10^{22}$	$E_{1,NFR}$	99-120	$n_{1,NFR}$	6.90-18.40	v_i
			$k_{20,NFR}$	$2.23x10^{2}$ - $8.89x10^{8}$	$E_{2,NFR}$	54-184	$n_{2,NFR}$	0.90-3.20	v_i
			$k_{10,FR}$	$1.20x10^{9}$ - $2.90x10^{16}$	$E_{1,FR}$	56-114	$n_{1,FR}$	9.30-13.30	v_i
			$k_{20,FR}$	$1.83x10^{1}$ - $1.62x10^{9}$	$E_{2,FR}$	42-193	$n_{2,FR}$	0.70-3.40	v_i
l et al. [27]	2 Consecutive reactions	2 Dynamic runs (5 and 10ºC/min)	k_{10}	1.69×10^{8}	E_1	135	n_1	1.00	v_i
			k_{20}	8.75×10^{9}	E_2	175	n_2	1.16	v_i
s study	2 Consecutive reactions	3 Dynamic runs (5, 10 and 20ºC/min) + 3 Dynamic+Isothermal runs (5, 10 and 20ºC/min-T_{final}: 260, 360 and 385ºC)	k_{10}	2.044×10^{11}	E_1	142.0	n_1	0.805	v_i
			k_{20}	3.247×10^{15}	E_2	217.5	n_2	1.246	v_i

NFR: Non-fire retardant

Table 5 Optimised parameters for combustion of FPUF

	Reaction 1	*Reaction 2*	*Reaction 3*
k_0 (s^{-1}·atm^{-b})	$4.053x10^{20}$	$5.086x10^{07}$	$6.663x10^{05}$
E (kJ mol^{-1})	237.9	103.5	120.1
n	2.003	0.778	1.025

v_{inf}	0.284	0.505	0.112
b	-	1.114	0.571
VC(%)		3.16	

Scheme	Experiments	Pre-exponential factor (s^{-1})		Activation Energy (kJ mol^{-1})		Reaction order		Reaction order oxygen	
1 Reaction	1 Dynamic run AIR (5ºC/min) (Compared with isothermal data)	k_{10}	$4.60x10^{6}$	E_1	97.4	n_1	1	b_1	-
3 Consecutive reactions	3 Dynamic runs AIR (5, 10 and 20ºC/min) Kinetic parameters for each heating rate	$k_{10,NFR}$	$5.97x10^{7}$ - $7.86x10^{17}$	$E_{1,NFR}$	96 - 295	$n_{1,NFR}$	10 - 25	$b_{1,NFR}$	-
		$k_{20,NFR}$	3.69 - $1.35x10^{2}$	$E_{2,NFR}$	27 - 62	$n_{2,NFR}$	0.5 - 1.5	$b_{2,NFR}$	-
		$k_{30,NFR}$	$4.96x10^{2}$- $6.02x10^{4}$	$E_{3,NFR}$	67 - 98	$n_{3,NFR}$	1.2 - 1.6	$b_{3,NFR}$	-
		$k_{10,FR}$	$2.02x10^{1}$ - $1.42x10^{21}$	$E_{1,FR}$	162 - 205	$n_{1,FR}$	11 - 19	$b_{1,FR}$	-
		$k_{20,FR}$	$8.17x10^{2}$ - $3.31x10^{3}$	$E_{2,FR}$	72 - 102	$n_{2,FR}$	1.3 - 2.2	$b_{2,FR}$	-
		$k_{30,FR}$	$1.65x10^{2}$ - $2.23x10^{2}$	$E_{3,FR}$	63 - 79	$n_{3,FR}$	1.2 - 1.3	$b_{3,FR}$	-
3 Consecutive reactions	4 Dynamic runs AIR (5, 10, 15 and 20ºC/min)	k_{10}	2.55×10^{12}	E_1	133.6	n_1	1	b_1	-
		k_{20}	3.26×10^{4}	E_2	81	n_2	1	b_2	-
		k_{30}	8.70×10^{8}	E_3	180	n_3	1	b_3	-
3 Consecutive reactions (1 Pyrolysis + 2 Combustions)	1 Dynamic run AIR (10ºC/min)	k_{10}	5.00×10^{5}	E_1	200	n_1	3	b_1	-
		k_{20}	2.00×10^{12}	E_2	155	n_2	1	b_2	1
		k_{30}	4.00×10^{13}	E_3	185	n_3	1	b_3	1
5 Reactions (2 Pyrolisis + 3 Combustions)	1 Dynamic run AIR (20ºC/min)	k_{10}	2.00×10^{11}	E_1	148	n_1	0.21	b_1	-
		k_{20}	1.58×10^{8}	E_2	124	n_2	1.14	b_2	-
		k_{30}	2.51×10^{15}	E_3	194	n_3	0.52	b_3	1
		k_{40}	2.51×10^{15}	E_4	195	n_4	0.52	b_4	1
		k_{50}	1.58×10^{15}	E_5	201	n_5	1.23	b_5	1
3 Consecutive reactions	6 Dynamic runs (5, 10 and 20ºC/min) + 6 Dynamic+Isothermal runs (5, 10 and 20ºC/min- T_{final}:260, 300 and 450ºC) 4:1 and 9:1 N_2:O_2	k_{10}	4.053×10^{20}	E_1	237.9	n_1	2.003	b_1	-
		k_{20}	5.086×10^{07}	E_2	103.5	n_2	0.778	b_2	1.114
		k_{30}	6.663×10^{05}	E_3	120.1	n_3	1.025	b_3	0.571

Table 6: Optimised parameters for combustion of FPUF.

R: Fire retardant